

**An eddy-resolving
physical-biological
model study study**

Y. Sasai et al.

Impact of physical processes on the phytoplankton blooms in the South China Sea: an eddy-resolving physical-biological model study

Y. Sasai¹, H. Sasaki², and K. J. Richards³

¹Research Institute for Global Change, Japan Agency for Marine-Earth Science and Technology, Yokohama, Japan

²Earth Simulator Center, Japan Agency for Marine-Earth Science and Technology, Yokohama, Japan

³International Pacific Research Center, SOEST, University of Hawaii, Honolulu, USA

Received: 27 December 2012 – Accepted: 14 January 2013 – Published: 31 January 2013

Correspondence to: Y. Sasai (ysasai@jamstec.go.jp)

Published by Copernicus Publications on behalf of the European Geosciences Union.

Title Page

Abstract

Introduction

Conclusions

References

Tables

Figures



Back

Close

Full Screen / Esc

Printer-friendly Version

Interactive Discussion



Abstract

An eddy-resolving coupled physical-biological ocean model has been employed to investigate the physical influences on phytoplankton blooms in the South China Sea during 2000–2007. The model captures the seasonal and interannual variability of surface chlorophyll distribution associated with mesoscale eddies, ocean circulation and upwelling generated by the monsoon winds. The model also reproduces the high chlorophyll distributions in two coastal upwelling regions: the northwestern Luzon in winter and the eastern coast of Vietnam in summer. To the northwest of Luzon, the monsoon driven-upwelling, anticyclonic eddies, and the intrusion of the Kuroshio have a large impact on the winter phytoplankton bloom. The model shows the winter phytoplankton bloom is induced by the shallow nutricline depth under the northeast monsoon. Strong vertical motions at the edge of anticyclonic eddies enhance the phytoplankton bloom and produce the filamentary structure. Off the eastern coast of Vietnam, the monsoon-driven upwelling and anticyclonic circulation control the high chlorophyll distribution in summer. During the southwest monsoon, strong offshore Ekman transport and upwelling occur and increase the surface chlorophyll. The high chlorophyll is advected from the coast to open ocean by the strong offshore circulation.

1 Introduction

The South China Sea (SCS) is influenced strongly by the monsoon system. The seasonal variation of monsoonal winds drives the surface oceanic circulation and upwelling in this region (e.g., Wyrтки, 1961; Shaw and Chao, 1994; Liu and Xie, 1999; Liu et al., 2002). The alternating monsoons in summer and winter lead to changes in the upper circulation system. In summer, the strong southwesterly winds drive an anticyclonic gyre in the SCS and result in localized upwelling off Vietnam (e.g., Kuo et al., 2000; Liu et al., 2002; Xie et al., 2003). In winter, the northeasterly winds force a cyclonic gyre

BGD

10, 1577–1604, 2013

An eddy-resolving physical-biological model study study

Y. Sasai et al.

Title Page

Abstract

Introduction

Conclusions

References

Tables

Figures

◀

▶

◀

▶

Back

Close

Full Screen / Esc

Printer-friendly Version

Interactive Discussion



in the SCS and drive the localized upwelling off the western Luzon (e.g., Qu, 2000; Liu et al., 2002).

The seasonal variation of the chlorophyll distribution in the SCS is very much affected by the alternating monsoon winds and resultant changes in ocean circulation.

The strong upwelling induced by the monsoon contributes to the high chlorophyll concentrations found in the areas off eastern Vietnam, and off western Luzon. During the southwest monsoon (May to September), the surface chlorophyll maximum occurs off the east coast of Vietnam. During the northeast monsoon (November to March), blooms appear off the northwest coast of Luzon, and the surface chlorophyll concentration in the upwelling regions is much reduced. Tang et al. (1999, 2004) investigated the effects of wind forcing on the phytoplankton blooms off the northwest of Luzon and off the east coast of Vietnam using hydrographic and satellite data. They indicated the phytoplankton blooms were related to upwelling, which brings nutrients to the surface waters. Wang et al. (2010) indicated that the winter phytoplankton bloom off the northwest of Luzon is primarily induced by both Ekman pumping-driven upwelling and upper mixed layer entrainment.

Interannual variations of the SCS circulation are related to both the El Niño Southern Oscillation (e.g., Kuo et al., 2004; Liu et al., 2004; Fang et al., 2006) and Indian Ocean Dipole (IOD) (Saji et al., 1999; Yang et al., 2010) the latter having a considerable impact on the southwest monsoon over the SCS. These climatic variations influence the monsoon winds, sea surface temperature (SST), and ocean circulation in the SCS, and the changed physical processes affect the biology. During El Niño years unusually high SST, weak wind stress, and weak Ekman pumping lead to a decrease of nutrients supply, resulting in a low chlorophyll concentration (Zhao and Tang, 2007; Jing et al., 2011). In 2007, a positive IOD and La Niña event acted to enhance the southwest monsoon over the SCS, with the enhanced wind increasing the upwelling and the phytoplankton bloom off the South Vietnam coast (Liu et al., 2012).

Mesoscale eddies are an important component of ocean dynamics in the SCS (Wang et al., 2003; Liu et al., 2008; Chen et al., 2011). They play an important role

BGD

10, 1577–1604, 2013

An eddy-resolving physical-biological model study study

Y. Sasai et al.

Title Page

Abstract

Introduction

Conclusions

References

Tables

Figures



Back

Close

Full Screen / Esc

Printer-friendly Version

Interactive Discussion



An eddy-resolving physical-biological model study study

Y. Sasai et al.

Title Page

Abstract

Introduction

Conclusions

References

Tables

Figures



Back

Close

Full Screen / Esc

Printer-friendly Version

Interactive Discussion



in the transport of heat, salt and biogeochemical tracers. Eddies affect the rates of nutrient supply to the euphotic zone through upwelling and downwelling, with a resultant change in phytoplankton productivity. To investigate the physical characters of mesoscale eddies in the SCS, many studies have been performed (e.g., Chi et al., 1998; Wang et al., 2003; Xiu et al., 2010; Zhuang et al., 2010). However, only limited studies, based on a few cruises data and satellite data, have focused on the impact of eddy activity on the phytoplankton productivity. Ning et al. (2004) observed high chlorophyll and primary production in cyclonic eddies and low chlorophyll and primary production in anticyclonic eddies. Chen et al. (2007) observed enhanced primary production in a cyclonic eddy in Luzon Strait. Lin et al. (2010) studied the phytoplankton bloom produced by an anticyclonic eddy injection in the oligotrophic area of the northern SCS. These studies, based on shipboard measurements, are limited both in time and space.

The physical-biological model provides a useful tool to address questions concerning the role of physical processes and their impact on the biogeochemical processes at different scales. Liu et al. (2002) demonstrated that the uplifted nutricline in association with the monsoon winds generated the observed level of chlorophyll in the SCS. They also simulated the high chlorophyll concentration off the east coast of Vietnam during the southwest monsoon and off the northwest of Luzon during the northeast monsoon. Liu and Chai (2009) investigated the seasonal and interannual variations of biogeochemical processes in the SCS. They showed the interannual variation of biological productivity is weaker than the seasonal variation. Xiu and Chai (2011) focused on the biogeochemical response to the modeled mesoscale eddies in the SCS. They compared the chlorophyll and new production in the cyclonic and anticyclonic eddies with the SCS basin mean. They showed cyclonic eddies enhance the chlorophyll and new production, and anticyclonic eddies reduce them.

In this study, we focus on the effect of monsoon variation and eddy activity on the phytoplankton blooms in the SCS using output of an eddy-resolving (0.1°) global physical-biological model (Sasai et al., 2006, 2010). The eddy-resolving model captures

mesoscale phenomena such as narrow boundary currents, filamentary structures, coastal upwelling, and eddy variability. We determine the seasonal variability of phytoplankton blooms influenced by the several scales of variability of physical processes and also examine the spatial response of phytoplankton blooms to interannual scale variability during the 2000–2007 period.

2 Model description

The physical model is the Ocean general circulation model For the Earth Simulator (OFES) (Masumoto et al., 2004), which is based on the Geophysical Fluid Dynamics Laboratory's Modular Ocean Model (MOM3) (Pacanowski and Griffies, 2000). The model domain covers 75° S to 75° N. The horizontal resolution is 0.1°. There are 54 vertical levels, with varying thickness between the levels from 5 m at the surface to 330 m at the maximum depth of 6065 m. The model topography is constructed from the 1/30° bathymetry dataset created by the OCCAM Project at the Southampton Oceanography Center. The model is spun-up for 50 years before initializing the biological fields.

The marine ecosystem model is a simple nitrogen-based four-compartment, NPZD (nitrate, phytoplankton, zooplankton and detritus), ecosystem model (Oschlies, 2001). The evolution of the biological tracer concentrations in the OFES is governed by an advection-diffusion equation with source and sink terms. The source and sink terms represent the biological activity. The details of the ecosystem model are described in Sasai et al. (2006, 2010). To establish a stable pattern of the biological fields, the biological model is incorporated into the physical model after the 50-yr spin-up with climatology and integrated for a further 5-yr period under the climatological monthly mean forcing. The variability of biological fields has no feedback on the physical fields. The biological fields in the last year of the coupled 5-yr integration are used as initial conditions for this simulation.

For the experiment reported here, the coupled physical-biological model (OFES-NPZD) is forced by the daily mean surface wind stress data of Quick Scatterometer

BGD

10, 1577–1604, 2013

An eddy-resolving physical-biological model study study

Y. Sasai et al.

Title Page

Abstract

Introduction

Conclusions

References

Tables

Figures



Back

Close

Full Screen / Esc

Printer-friendly Version

Interactive Discussion



An eddy-resolving physical-biological model study study

Y. Sasai et al.

Title Page

Abstract

Introduction

Conclusions

References

Tables

Figures



Back

Close

Full Screen / Esc

Printer-friendly Version

Interactive Discussion

east coast of Vietnam and drive the anticyclonic gyre (Fig. 2) in the southern basin of SCS. The coastal upwelling brings cold, nutrient rich close to the surface. There is large vertical nitrate flux ($> 4 \text{ mmol N m}^{-2} \text{ d}^{-1}$), which induces a phytoplankton bloom with chlorophyll concentrations in excess of 0.3 mg m^{-3} . An offshore current (Fig. 2), which is a part of an anticyclonic gyre, transports the high chlorophyll concentration from the coast to the open ocean. In the pelagic ocean, excluding the coast and upwelling regions, the simulated chlorophyll concentration is mostly below 0.2 mg m^{-3} , similar to that seen in SeaWiFS.

In December, northeasterly winds are dominant over the SCS, and change the surface circulation system (Fig. 2). The cyclonic circulation is dominant in the SCS basin. The reversed wind changes the location of the upwelling regions. The upward Ekman pumping area from the southern SCS to the western Luzon inputs high nitrate waters into the surface layer. The model clearly captures the high chlorophyll ($> 0.3 \text{ mg m}^{-3}$) distribution off the northwestern Luzon as seen in SeaWiFS data. The high chlorophyll area extends from the northwestern Luzon to open ocean (500 km). The thermocline depth is shallow ($< 75 \text{ m}$ depth) and the high nitrate ($> 1 \text{ mmol N m}^{-3}$) waters lift up from the subsurface layer. The vertical nitrate flux is also strong ($> 4 \text{ mmol N m}^{-2} \text{ d}^{-1}$), and the high surface chlorophyll conditions are maintained by the nitrate supply from subsurface layer in the northwestern Luzon. The strong Kuroshio inflow also effects on the spreading of surface chlorophyll distribution. Outside of the coastal and upwelling regions, the simulated chlorophyll concentration is again below 0.2 mg m^{-3} .

In general, the seasonal variability of the observed surface chlorophyll distribution is reproduced in the model. In particular, the model captures the high chlorophyll distribution in the coastal upwelling regions, which is strongly influenced by the monsoon winds, as well as the low chlorophyll in the open ocean. However, the model underestimates chlorophyll concentrations along the coast of southwestern China, southern Vietnam, and Philippines Islands. This is because the coupled physical-biological model does not include nitrate input with river runoff. Additionally, since the parameter

values for phytoplankton growth based on open ocean values, they may not be suitable for the coastal environment (e.g., Liu et al., 2002; Liu and Chai, 2009).

To focus on the seasonal variability at two sites strongly affected by changes to the upwelling, Fig. 3 shows the box-averaged monthly mean surface chlorophyll from observations and model together with the model isotherm depth, nitrate and nitrate flux, for regions off the northwestern Luzon and east coast of Vietnam, labeled L and V, respectively (see Fig. 1). The SeaWiFS shows phytoplankton blooms off the northwestern Luzon, and high chlorophyll concentrations along the coast of southern Vietnam, southwestern China, and Philippines Islands in response to the induced upwelling. The wind field is reverse over the SCS, and the upwelling region is formed in the right of the wind in the Northern Hemisphere. The seasonal variability of the simulated surface chlorophyll concentration is similar to that found in SeaWiFS data for each box. In Box L, the peak in the simulated surface chlorophyll concentration (0.4 mg m^{-3}) in December/January is consistent with the shallow thermocline depth (70 m), the high nitrate concentration ($> 0.5 \text{ mmol N m}^{-3}$) in the upper 73 m, and the strong vertical nitrate flux ($> 0.5 \text{ mmol N m}^{-2} \text{ d}^{-1}$). In Box V, the observed surface chlorophyll concentration shows a peak in August (0.2 mg m^{-3}). The model also shows a peak in surface chlorophyll in August at a time of a shallowing thermocline, a high vertical nitrate flux and associated increased nitrate levels induced by the monsoon-driven upwelling. Surface nutrient levels become depleted and the surface chlorophyll reduces despite the continuing elevated levels of the depth-integrated nitrate. The observed surface chlorophyll shows an increase in November and December. This is caused by two unusually high chlorophyll events occurring at the end of 2005 and 2007, respectively, which are not captured by the model (see Fig. 4c – the reason for these events is unclear).

3.2 Interannual variability of chlorophyll in the two upwelling regions

The timing of the mean seasonal variation of surface chlorophyll off northwestern Luzon (Box L) and the east coast of Vietnam (Box V) is very much influenced by the seasonal variation of the monsoon winds (Fig. 2). The relative amplitude of the seasonal cycle,

BGD

10, 1577–1604, 2013

An eddy-resolving physical-biological model study study

Y. Sasai et al.

Title Page

Abstract

Introduction

Conclusions

References

Tables

Figures

◀

▶

◀

▶

Back

Close

Full Screen / Esc

Printer-friendly Version

Interactive Discussion



BGD

10, 1577–1604, 2013

An eddy-resolving
physical-biological
model study study

Y. Sasai et al.

Title Page

Abstract

Introduction

Conclusions

References

Tables

Figures



Back

Close

Full Screen / Esc

Printer-friendly Version

Interactive Discussion



compared to interannual variations, at each location is, however, very different. The time series of monthly mean surface chlorophyll concentrations of SeaWiFS and OFES and wind stress averaged for Box L and V during 2000–2007 is shown in Fig. 4. In Box L the signal is dominated by the seasonal cycle with the peak in chlorophyll occurring close to the year boundary. There is interannual variability in the strength of the peak values in both SeaWiFS and OFES. OFES tends to overestimate the peak but it does capture the observed relatively high peaks around January 2002, 2004 and 2005. The exception is the observed high peak around January 2006, which is not found in the OFES time series. The vertical distribution of properties averaged over Box L is shown in Fig. 5. Again the seasonal cycle dominates with the bloom in chlorophyll occurring at a time when the thermocline and nutricline are both shallow (the shallowing being consistent with the positive upward velocity towards the end of the year). A subsurface maximum in chlorophyll lingers for a few months after the bloom. The depth/time plot of chlorophyll also shows the interannual variations in surface chlorophyll are, in general, representative of the variations with depth. The exception is again around January 2006. Also shown in Fig. 4 is the monthly averaged wind stress over the region. There is no obvious correlation between the strength of the upwelling winds preceding the winter bloom and the strength of the bloom. Instead interannual variability in the chlorophyll concentration is most affected by eddy variability and the intrusion of Kuroshio waters into the SCS. This is looked at in detail in Sect. 3.3.

Off the coast of Vietnam (Box V) seasonal variability is less dominant (Fig. 4c), although there is a peak in surface chlorophyll in most years around August (as seen in the seasonal mean, Fig. 3). The exception is 2004 when there is no significant peak in OFES (and a reduced seasonal cycle in SeaWiFS). Referring to the depth/time plots in Fig. 6, we see there was a much-reduced seasonal variation in the depth of the thermocline and nutricline during 2004. There was a modest reduction in the strength of the summer monsoon winds (particularly the eastward component of wind stress; Fig. 4d) during 2004, which may account for the reduced bloom. The highest chlorophyll values are found at a subsurface maximum that varies in depth between 40–60 m depth

An eddy-resolving physical-biological model study study

Y. Sasai et al.

[Title Page](#)[Abstract](#)[Introduction](#)[Conclusions](#)[References](#)[Tables](#)[Figures](#)[⏪](#)[⏩](#)[◀](#)[▶](#)[Back](#)[Close](#)[Full Screen / Esc](#)[Printer-friendly Version](#)[Interactive Discussion](#)

surface chlorophyll concentration is small ($< 0.1 \text{ mg m}^{-3}$) in the center of the anticyclonic eddy and is high ($> 0.2 \text{ mg m}^{-3}$) at the edge of eddy, especially, on the southern side ($> 0.6 \text{ mg m}^{-3}$). On the western side of Luzon (south of the anticyclonic eddy), the thermocline and nutricline are shallow because of the strong northwesterly winds.

In the center of the anticyclonic eddy, the nitrate concentration remains at a low level ($< 0.1 \text{ mmol N m}^{-3}$). When the eddy arrives in the high nitrate area, the high nitrate water is drawn out along the southern edge of the eddy. A filament of high chlorophyll concentration is stretched out along the south edge of anticyclonic eddy associated with the high nitrate water. There are large upward and downward motions associated with the eddy.

Figure 8 shows the vertical distribution of chlorophyll concentration, nitrate concentration with potential density, and vertical velocity along the center of anticyclonic eddy (dashed line in Fig. 7d). In November 2003, high chlorophyll concentrations ($> 0.4 \text{ mg m}^{-3}$) occur in the subsurface layer (50–75 m depth) at the south edge (20° N) of the anticyclonic eddy. Potential density and nutrient contours are pushed down by the presence of the eddy such that at the center of the eddy low nitrate ($< 0.1 \text{ mmol N m}^{-3}$) water reaches down to 150 m depth. In December 2003, the chlorophyll concentration in the south edge of anticyclonic eddy increases ($> 0.6 \text{ mg m}^{-3}$) because the high nitrate water is uplifted along the steep slope of potential density (20° N) by the strong upward vertical velocity ($> 10 \text{ m day}^{-1}$) induced by the eddy. In January 2004, the slope of potential density surfaces is increased, and the high nitrate water is brought close to the surface layer. A narrow filament shape of high chlorophyll is formed at the south edge of anticyclonic eddy (19° N). In February 2004, the high nitrate water ($> 2.0 \text{ mmol N m}^{-3}$) reaches the surface and the chlorophyll concentration is over 1.5 mg m^{-3} at the south edge of eddy.

In the period 2000–2007, the model captures two incidences (in 2003–2004 and 2004–2005) of the separated anticyclonic eddy from the Kuroshio passing through the region during the winter (December–February) phytoplankton bloom in the northern SCS. By overlapping with the bloom season, the steep slope of potential density with

the vertical velocity enhances the chlorophyll concentration in the south edge of anticyclonic eddy and the areal average of surface chlorophyll in Box L (Fig. 4a). When the eddy passes through the northern SCS before or after phytoplankton bloom (as in 2000–2001, 2002–2003), the influence of the eddy on the phytoplankton bloom is small and the areal average of surface chlorophyll in Box L is relatively small (Fig 4a). In winters with no detached eddy (2001–2002, 2005–2006, 2006–2007), the intrusion of the Kuroshio can still impact the chlorophyll concentration along its southern edge (in a manner similar to that of the detached anticyclonic eddy). The impact in 2001–2002 was particularly strong (Fig. 4a).

3.4 Vietnam coast

Off the east coast of Vietnam, the pattern of the phytoplankton bloom during the southwest monsoon (July–August) is largely influenced by the coastal upwelling and offshore advection by an anticyclonic circulation. The OFES reproduces a similar pattern in surface chlorophyll during this period to that observed by satellites (Tang et al., 2004). Figure 9 shows the variability of physical and biological fields from June 2002 to September 2002, which is typical of most years in the OFES (strongest southwesterly wind in Fig. 4d). The SSHA and surface horizontal velocity fields show the presence of a strong anticyclonic gyre off the east coast of Vietnam (Fig. 9a). In June 2002, the current along the east coast of Vietnam is northward. The chlorophyll concentration near the east coast of Vietnam at around 12° N is high associated with the high nitrate supply by the coastal upwelling. From July 2002 to September 2002, the anticyclonic gyre is dominant during the southwesterly monsoon winds. The coastal jet separates from the Vietnam coast at around 12° N and flows to the northeast. To the north of the anticyclonic gyre, there is a general increase in the nitrate concentration at 73 m depth (associated with a shallowing thermocline and nutricline), but note that the higher chlorophyll levels are restricted to the northern edge of the anticyclonic circulation. Within the anticyclonic gyre, the thermocline and nutricline are depressed and the nitrate concentration is low ($< 0.1 \text{ mmol N m}^{-3}$). The surface chlorophyll concentration remains low ($< 0.2 \text{ mg m}^{-3}$).

An eddy-resolving physical-biological model study study

Y. Sasai et al.

Title Page

Abstract

Introduction

Conclusions

References

Tables

Figures



Back

Close

Full Screen / Esc

Printer-friendly Version

Interactive Discussion



An eddy-resolving physical-biological model study study

Y. Sasai et al.

Title Page

Abstract

Introduction

Conclusions

References

Tables

Figures



Back

Close

Full Screen / Esc

Printer-friendly Version

Interactive Discussion



Figure 10 shows the vertical distribution of chlorophyll concentration, nitrate concentration with potential density, and vertical velocity across the anticyclonic gyre along 111° E. Associated with the variation of anticyclonic gyre, the pattern of surface chlorophyll is changed. In June 2002, a subsurface maximum in chlorophyll (50–75 m depth) appears in the northern side of anticyclonic gyre (12° N– 15° N) and continues through September. This is in response to the shallowing thermocline and nutricline north of 12° N. In July 2002, the high chlorophyll concentration ($> 0.6 \text{ mg m}^{-3}$) is brought to the surface at the northern edge of anticyclonic circulation (11° N– 13° N). In August 2002, the slope of the potential density surfaces is increased by the strengthening of the anticyclonic circulation and there is a strong upward motion ($> 10 \text{ m day}^{-1}$) (Fig. 9d). By September 2002, the current is straight flowing from the west (coast) to east (open ocean) around 11° N. The chlorophyll concentration at the northern edge of the anticyclonic circulation (11° N) is decreased because the reduced nitrate supply to the surface layer, but the subsurface chlorophyll maximum layer (around 50 m depth) to the north of 11° N is maintained, together with the shallow thermocline and nutricline.

In the model, the interannual variability of surface chlorophyll distribution off the east coast of Vietnam is small. The model reproduces the anticyclonic gyre during summer monsoon (July–August) and the interannual variation is small in the period 2000–2007. The reason for the small variation of physical fields (circulation pattern and upwelling system) off the east coast of Vietnam may be the small interannual variability of wind stress field (Fig. 4d).

4 Conclusions

Climatic variation in the upper ocean of the SCS is primarily controlled by the monsoon. We have investigated the impact of this variation on the phytoplankton blooms using an eddy-resolving physical-biological model. For the period from 2000 to 2007, the model clearly reproduces the seasonal cycle of surface chlorophyll concentration, which is caused by the seasonal variation of physical processes (upwelling and surface

An eddy-resolving physical-biological model study study

Y. Sasai et al.

[Title Page](#)[Abstract](#)[Introduction](#)[Conclusions](#)[References](#)[Tables](#)[Figures](#)[Back](#)[Close](#)[Full Screen / Esc](#)[Printer-friendly Version](#)[Interactive Discussion](#)

ocean circulation drives by the surface winds, and the thermocline depth). The spatial distribution of surface chlorophyll concentration is consistent with the distribution of the thermocline depth and subsurface nitrate concentration. In particular, the seasonal variability of surface chlorophyll concentration in the two upwelling regions (northwestern Luzon, and east coast of Vietnam) is largely influenced by the monsoon winds. The phytoplankton bloom peaks in two upwelling regions similar to that observed in SeaWiFS data. The shallowest period of nutricline depth is also consistent with the phytoplankton bloom peaks. The nitrate supply by the shoaling of nutricline depth mainly controls the phytoplankton bloom.

To the northwest of Luzon, the winter phytoplankton bloom occurs due to nutrients supplied from the subsurface layer. The strong northeasterly winds blow parallel to the west coast of Luzon, and strong offshore Ekman transport and upwelling occur. The nutricline depth is shallowed by the upwelling and high nutrient waters are supplied by the winter mixing for the phytoplankton blooms. This result indicates the same winter phytoplankton bloom mechanism investigated using observed data (Chen et al., 2006). In addition to this mechanism, OFES also shows the role of anticyclonic eddies and the intrusion of the Kuroshio on the winter phytoplankton bloom. The timing of these events is important. When the anticyclonic eddy separated from the Kuroshio passes over the region during the winter phytoplankton bloom the overall strength of the bloom is increased as a filamentary structure on the southern edge of the eddy. Off the east coast of Vietnam the phytoplankton bloom occurs in the boreal summer. The mechanism of the summer phytoplankton bloom has been described by Tang et al. (2004) using satellite data and ship measurements. Near the Mekong River mouth, the river-discharged nutrients initiate the phytoplankton plume. The strong southwesterly winds blow parallel to coastline and strong offshore Ekman transport and upwelling occur. The upwelled nutrients support a strong phytoplankton bloom. The phytoplankton bloom is advected offshore into the SCS by a strong anticyclonic circulation. OFES captures the detailed nutrient dynamics and phytoplankton bloom during the southwest monsoon, except the river discharge of nutrients. The interannual variability of chlorophyll off the east coast

An eddy-resolving physical-biological model study study

Y. Sasai et al.

Title Page

Abstract

Introduction

Conclusions

References

Tables

Figures

◀

▶

◀

▶

Back

Close

Full Screen / Esc

Printer-friendly Version

Interactive Discussion



of Vietnam is not large in the OFES during 2000–2007. The model fails to capture the two large observed events in summer/fall 2005, and summer/fall 2007 (Fig. 4c). Liu et al. (2012) showed the high chlorophyll concentration off the east coast of Vietnam is enhanced by the positive IOD of 2007 and the Madden–Julian Oscillation (MJO) events using the satellite data. The simulated chlorophyll concentration in 2007 is not large because the reproduced upwelling in the OFES is not much difference from other years (Fig. 6d).

Acknowledgement. We thank Yukio Masumoto, Akio Ishida, and Takashi Kagimoto for their collaborations in extending the OFES model for biological research. The QSCAT product of J-OFURO was obtained from Kunio Kutsuwada. Using ocean color satellite data was obtained from Kosei Sasaoka. OFES simulations were conducted on the Earth Simulator under support of JAMSTEC. This work was partly supported by a Grand-in-Aid for Scientific Research (22106006 and that on Innovative Areas 2205) from MEXT of Japan.

References

- Chen, C. C., Shiah, F. K., Chung, S. W., and Liu, K. K.: Winter phytoplankton blooms in the shallow mixed layer of the South China Sea enhanced by upwelling, *J. Mar. Systems*, 59, 97–110, 2006.
- Chen, G., Hou, Y., and Chu, X.: Meoscale eddies in the South China Sea: mean properties, spatiotemporal variability, and impact on thermocline structure, *J. Geophys. Res.*, 116, C06018, doi:10.1029/2010JC006716, 2011.
- Chen, Y.-L., Chen, H.-Y., Lin, I.-I., Lee, M.-A., and Chang, J.: Effects of cold eddy on phytoplankton production and assemblage in Luzon Strait bordering the South China Sea, *J. Oceanogr.*, 63, 671–683, doi:10.1007/s10872-007-0059-9, 2007.
- Chi, P. C., Chen, Y., and Lu, S.: Wind-driven South China Sea deep basin warm-core/cold eddies, *J. Oceanogr.*, 54, 347–360, doi:10.1007/BF02742619, 1998.
- Cloern, J. E., Grenz, C., and Vidergar-Lucas, L.: An empirical model of the phytoplankton chlorophyll: carbon ratio-the conversion factor between productivity and growth rate. *Limnol. Oceanogr.*, 40, 1313–1321, 1995.

An eddy-resolving physical-biological model study study

Y. Sasai et al.

Title Page

Abstract

Introduction

Conclusions

References

Tables

Figures

◀

▶

◀

▶

Back

Close

Full Screen / Esc

Printer-friendly Version

Interactive Discussion



- Fang, G., Chen, H., Wei, Z., Wang, Y., Wang, X., and Li, C.: Trends and interannual variability of the South China Sea surface winds, surface height, and surface temperature in the recent decade, *J. Geophys. Res.*, 111, C11S16, doi:10.1029/2005JC003276, 2006.
- Hu, J., Kawamura, H., Hong, H., and Qi, Y.: A review on the currents in the South China Sea: seasonal circulation, South China Sea warm current and Kuroshio intrusion, *J. Oceanogr.*, 56, 607–624, 2000.
- Jing, Z. Y., Qi, Y. Q., and Du, Y.: Upwelling in the continental shelf of northern South China Sea in recent years, *J. Geophys. Res.*, 116, C02033, doi:10.1029/2010JC006598, 2011.
- Kalnay, E., Kanamitsu, M., Kistler, R., Collins, W., Deaven, D., Gandin, L., Iredell, M., Saha, S., White, G., Woollen, J., Zhu, Y., Chelliah, M., Ebisuzaki, W., Higgins, W., Janowiak, J., Mo, K. C., Ropelewski, C., Leetmaa, A., Reynolds, R., and Jenne, R.: The NCEP/NCAR 40-year reanalysis project, *Bull. Am. Meteorol. Soc.*, 77, 437–471, 1996.
- Kuo, N. J., Zheng, Q. A., and Ho, C. B.: Satellite observation of upwelling along the western coast of the South China Sea, *Remote Sens. Environ.*, 74, 463–470, 2000.
- Kuo, N. J., Zheng, Q. A., and Ho, C. B.: Response of Vietnam coastal upwelling to the 1997–1998 ENSO event observed by multisensory data, *Remote Sens. Environm.*, 89, 106–115, 2004.
- Li, L., Nowlin Jr., W. D., and Jilan, S.: Anticyclonic rings from the Kuroshio in the South China Sea, *Deep-Sea Res. Pt. I*, 45, 1469–1482, 1998.
- Lin, I.-I., Lien, C.-C., Wu, C.-R., Wong, G. T. F., Huang, C.-W., and Chiang, T.-L.: Enhanced primary production in the oligotrophic South China Sea by eddy injection in spring, *Geophys. Res. Lett.*, 37, L16602, doi:10.1029/2010GL043872, 2010.
- Liu, G. and Chai, F.: Seasonal and interannual variability of primary and export production in the South China Sea: a three-dimensional physical-biogeochemical model study, *ICES J. Mar. Sci.*, 66, 420–431, doi:10.1093/icesjms/fsn219, 2009.
- Liu, K. K., Chao, S. Y., Shaw, P. T., Gong, G. C., Chen, C. C., and Tang, T. Y.: Monsoon-forced chlorophyll distribution and primary production in the South China Sea: observations and a numerical study, *Deep-Sea Res. Pt. I*, 49, 1387–1412, 2002.
- Liu, Q., Jiang, X., Xie, S.-P., and Liu, T.: A gap in the Indo-Pacific warm pool over the South China Sea in boreal winter: seasonal development and interannual variability, *J. Geophys. Res.*, 109, C07012, doi:10.1029/2003JC002179, 2004.
- Liu, Q., Kaneko, A., and Jilan, S.: Recent progress in studies of the South China Sea circulation, *J. Oceanogr.*, 64, 753–762, doi:10.1007/s10872-008-0063-8, 2008.

An eddy-resolving physical-biological model study study

Y. Sasai et al.

Title Page

Abstract

Introduction

Conclusions

References

Tables

Figures

◀

▶

◀

▶

Back

Close

Full Screen / Esc

Printer-friendly Version

Interactive Discussion

- Liu, W. T., and Xie, X.: Space-based observations of the seasonal changes of the South Asian Monsoons and oceanic response, *Geophys. Res. Lett.*, 26, 1473–1476, doi:10.1029/1999GL900289, 1999.
- Liu, X., Wang, J., Cheng, X., and Du, Y.: Abnormal upwelling and chlorophyll-*a* concentration off South Vietnam in summer 2007, *J. Geophys. Res.*, 117, C07021, doi:10.1029/2012JC008052, 2012.
- Masumoto, Y., Sasaki, H., Kagimoto, T., Komori, N., Ishida, A., Sasai, Y., Miyama, T., Motoi, T., Mitsudera, H., Takahashi, K., and Sakuma, H.: A fifty-year-eddy-resolving simulation of the world ocean: Preliminary outcomes of OFES (OGCM for the Earth Simulator), *J. Earth Simulator*, 1, 35–56, 2004.
- Ning, X., Chai, F., Xue, H., Cai, Y., Liu, C., and Shi, J.: Physical-biological oceanographic coupling influencing phytoplankton and primary production in the South China Sea, *J. Geophys. Res.*, 109, C10005, doi:10.1029/2004JC002365, 2004.
- Oschlies, A.: Model-derived estimates of new production: new results point towards lower values, *Deep-Sea Res Pt. II*, 48, 2173–2197, 2001.
- Pacanowski, R. C., and Griffies, S. M.: *MOM 3.0 Manual*, Geophysical Fluid Dynamics Laboratory/National Oceanic and Atmospheric Administration, 680 pp., 2000.
- Qu, T.: Upper-layer circulation in the South China Sea, *J. Phys. Oceanogr.*, 30, 1450–1460, 2000.
- Qu, T., Mitsudera, H., and Yamagata, T.: Intrusion of the North Pacific waters into the South China Sea, *J. Geophys. Res.*, 15, 6415–6424, 2000.
- Saji, N. H., Goswami, B. N., Vinayachandran, P. N., and Yamagata, T.: A dipole mode in the tropical Indian Ocean, *Nature*, 401, 360–363, 1999.
- Sasai, Y., Ishida, A., Sasaki, H., Kawahara, S., Uehara, H., and Yamanaka, Y.: A global eddy-resolving coupled physical and biological model: physical influences on a marine ecosystem in the North Pacific, *Simulation*, 82, 467–474, 2006.
- Sasai, Y., Richards, K. J., Ishida, A., and Sasaki, H.: Effects of cyclonic mesoscale eddies on the marine ecosystem in the Kuroshio Extension region using an eddy-resolving coupled physical-biological model, *Ocean Dynam.*, 60, 693–704, doi:10.1007/s10236-010-0264-8, 2010.
- Shaw, P. T. and Chao, S. Y.: Surface circulation in the South China Sea, *Deep-Sea Res. Pt. I*, 41, 1663–1683, 1994.

An eddy-resolving physical-biological model study study

Y. Sasai et al.

Title Page

Abstract

Introduction

Conclusions

References

Tables

Figures

◀

▶

◀

▶

Back

Close

Full Screen / Esc

Printer-friendly Version

Interactive Discussion



Tang, D. L., Ni, I. H., Kestner, D. R., and Müller-Kargen, F. E.: Remote sensing observations of winter phytoplankton blooms southeast of the Luzon Strait in the South China Sea, *Mar. Ecol. Prog. Ser.*, 191, 43–51, 1999.

Tang, D. L., Kawamura, H., Dien, T. V., and Lee, M. A.: Offshore phytoplankton biomass increase and its oceanographic causes in the South China Sea, *Mar. Ecol. Prog. Ser.*, 268, 31–41, 2004.

Wang, G., Su, J., and Chu, P. C.: Mesoscale eddies in the South China Sea detected from the altimeter data, *Geophys. Res. Lett.*, 30, 2121, doi:10.1029/2003GL018532, 2003.

Wang, J. J., Tang, D. L., and Sui, Y.: Winter phytoplankton bloom induced by subsurface upwelling and mixed layer entrainment southwest of Luzon Strait, *J. Mar. Systems*, 83, 141–149, 2010.

Wyrtki, K.: Physical oceanography of the south-east Asian waters, NAGA Report Vol. 2, Scientific Results of Marine Investigations of the South China Sea and the Gulf of Thailand, Scripps Institution of Oceanography, La Jolla, CA, 195 pp., 1961.

Xie, S.-P., Xie, Q., Wang, D., and Liu, W. T.: Summer upwelling in the South China Sea and its role in regional climate variations, *J. Geophys. Res.*, 108, 3261, doi:10.1029/2003JC001867, 2003.

Xiu, P. and Chai, F.: Modeled biogeochemical responses to mesoscale eddies in the South China Sea, *J. Geophys. Res.*, 116, C10006, doi:10.1029/2010JC006800, 2011.

Xiu, P., Chai, F., Shi, L., Xue, H., and Chao, Y.: A census of eddy activities in the South China Sea during 1993–2007, *J. Geophys. Res.*, 115, C03012, doi:10.1029/2009JC005657, 2010.

Yang, J. L., Liu Q. Y., and Liu, Z. Y.: Linking observations of the Asian monsoon to the Indian Ocean SST: possible roles of Indian Ocean basin mode and dipole mode, *J. Clim.*, 23, 5889–5902, doi:10.1175/2010JC12962.1, 2010.

Zhao, H. and Tang, D. L.: Effects of 1998 El Niño on the distribution of phytoplankton in the South China Sea, *J. Geophys. Res.*, 112, C02017, doi:10.1029/2006JC003536, 2007.

Zhuang, W., Xie, S.-P., Wand, D., Taguchi, B., Aiki, N., and Sasaki, H.: Interseasonal variability in sea surface height over the South China Sea, *J. Geophys. Res.*, 115, C04010, doi:10.1029/2009JC005647, 2010.

An eddy-resolving physical-biological model study

Y. Sasai et al.

Title Page

Abstract

Introduction

Conclusions

References

Tables

Figures

◀

▶

◀

▶

Back

Close

Full Screen / Esc

Printer-friendly Version

Interactive Discussion

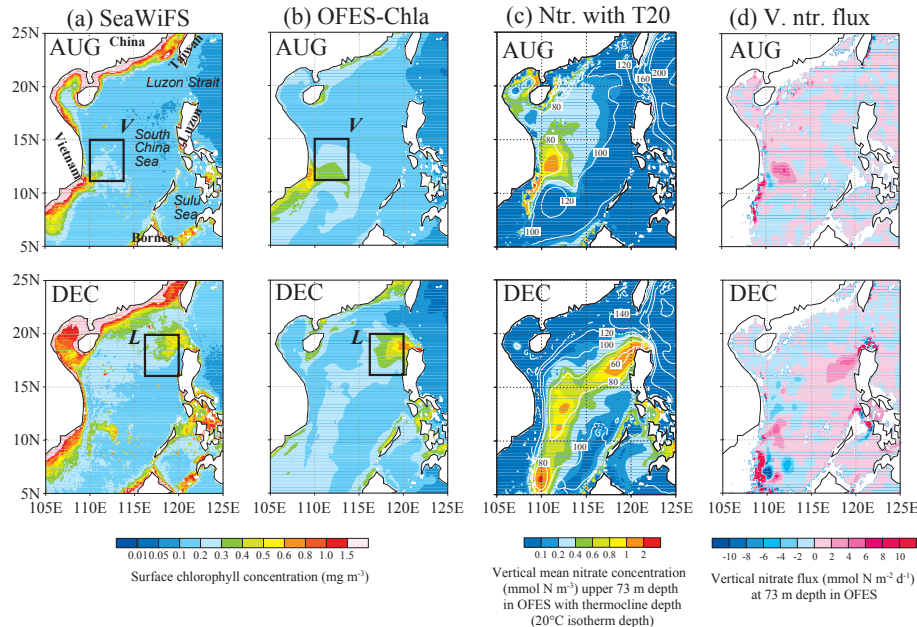


Fig. 1. Climatological monthly mean surface chlorophyll concentration (mg m^{-3}) during 2000–2007 from **(a)** SeaWiFS and **(b)** OFES, **(c)** vertical mean nitrate concentration (mmol N m^{-3}) upper 73 m depth with thermocline depth (contour in m, 20° isotherm depth), and **(d)** vertical nitrate flux ($\text{mmol N m}^{-2} \text{day}^{-1}$) at 73 m depth in OFES. Boxes off northwestern Luzon, and southeast Vietnam are upwelling regions (L and V) discussed in the text. Positive nitrate flux in **(d)** is upward. Negative nitrate flux in **(d)** is opposite sign.

An eddy-resolving physical-biological model study

Y. Sasai et al.

Title Page

Abstract

Introduction

Conclusions

References

Tables

Figures

◀

▶

◀

▶

Back

Close

Full Screen / Esc

Printer-friendly Version

Interactive Discussion

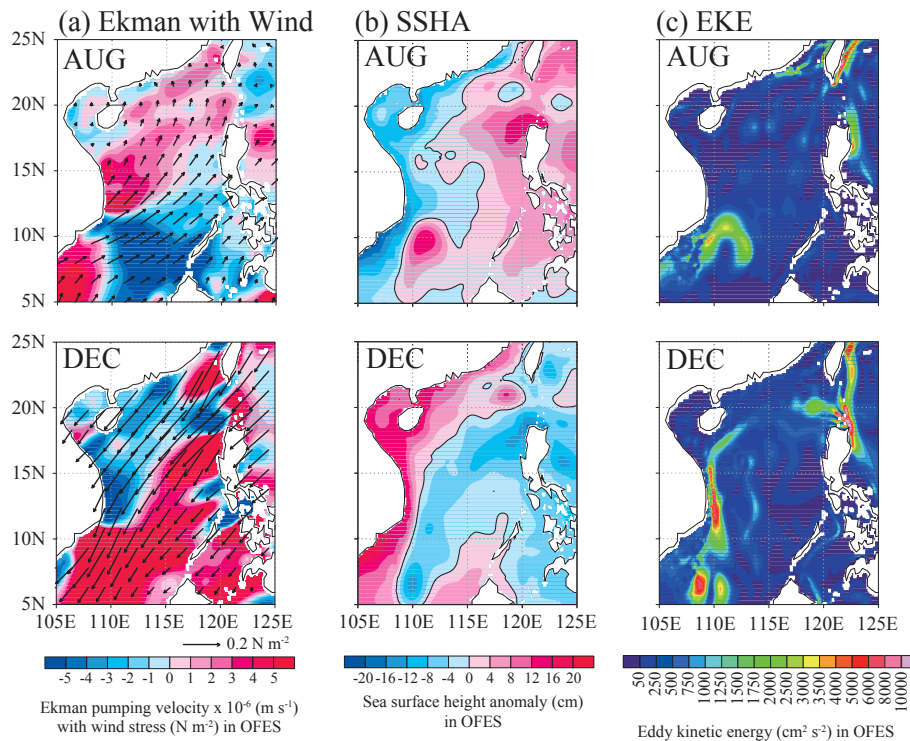


Fig. 2. Climatological monthly mean (a) Ekman pumping ($\times 10^{-6} \text{ m s}^{-1}$) with wind stress (N m^{-2}), (b) sea surface height anomaly (cm), and (c) eddy kinetic energy ($\text{cm}^2 \text{ s}^{-2}$) in the surface layer in OFES. Contour line in (b) is 0 cm.

An eddy-resolving physical-biological model study

Y. Sasai et al.

Title Page

Abstract

Introduction

Conclusions

References

Tables

Figures



Back

Close

Full Screen / Esc

Printer-friendly Version

Interactive Discussion

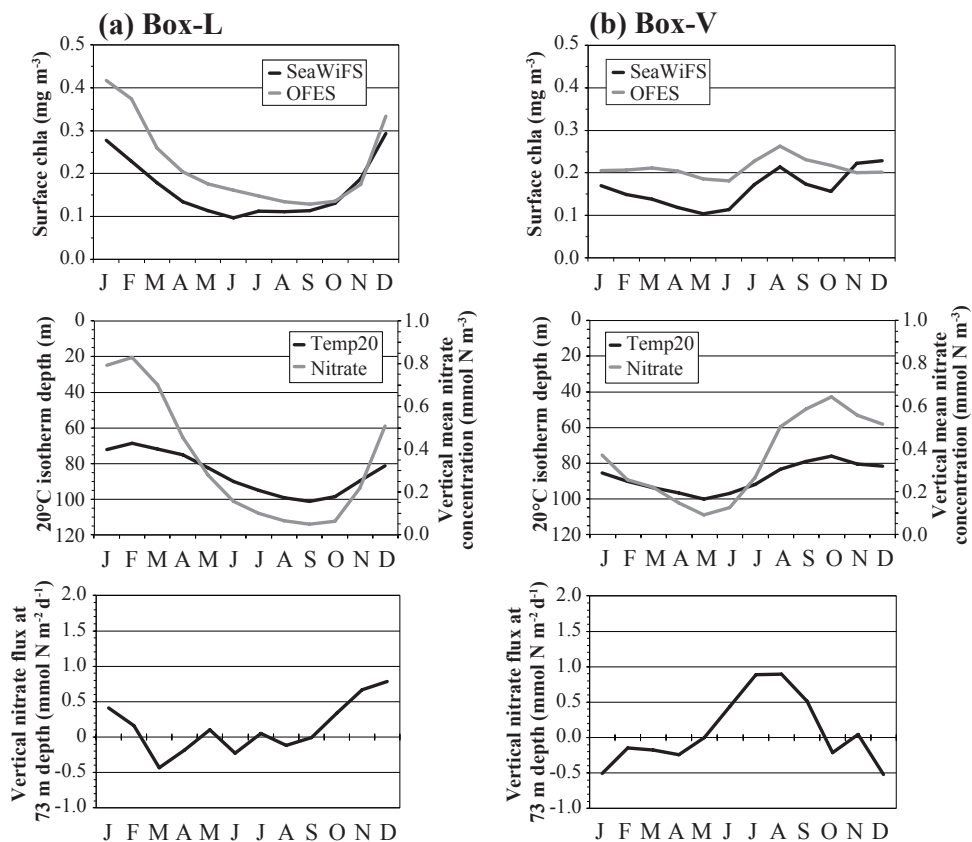


Fig. 3. Time series of climatological monthly mean surface chlorophyll concentrations, thermocline depth, vertical mean nitrate concentration, and vertical nitrate flux at 73 m depth averaged for each upwelling region of Fig. 1: **(a)** Box-L of northwestern Luzon (16° N–20° N, 116° E–120° E) and **(b)** Box-V of southeast Vietnam (11° N–15° N, 110° E–114° E).

An eddy-resolving physical-biological model study

Y. Sasai et al.

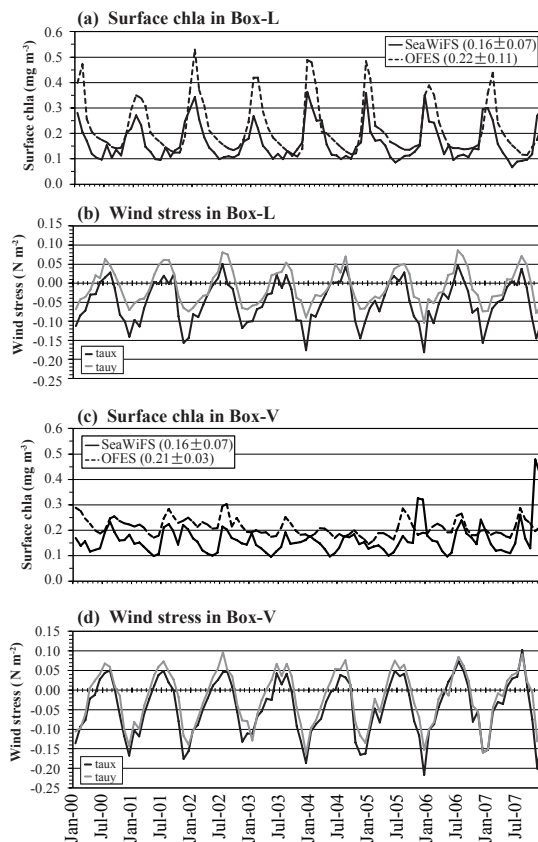


Fig. 4. Time series of monthly mean surface chlorophyll concentrations (mg m^{-3}) and wind stress (N m^{-2}) averaged for each upwelling region of Fig. 1 during 2000–2007 in (a, b) Box-L and (c, d) Box-V.

Title Page

Abstract

Introduction

Conclusions

References

Tables

Figures



Back

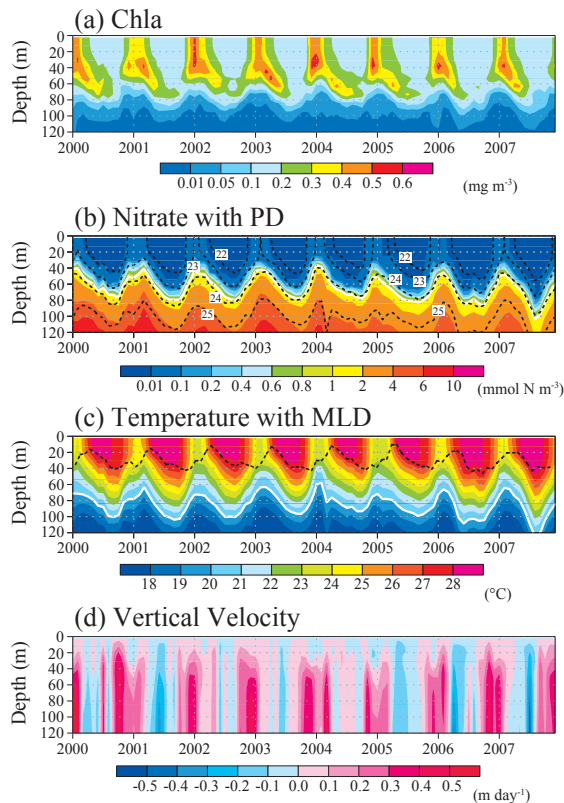
Close

Full Screen / Esc

Printer-friendly Version

Interactive Discussion



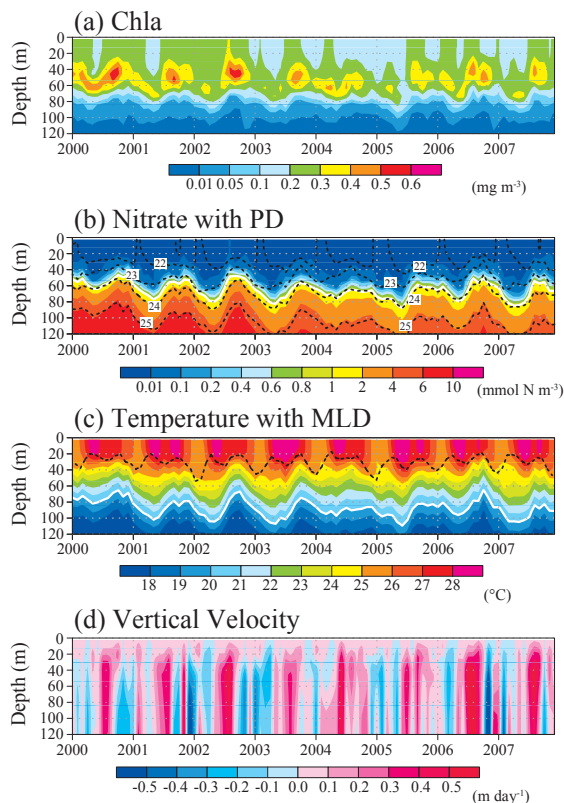


Box-L (16°N–20°N, 116°E–120°E)

Fig. 5. Time series of simulated vertical distribution of **(a)** chlorophyll concentration (mg m^{-3}), **(b)** nitrate concentration (mmol N m^{-3}) with potential density (dashed line), **(c)** temperature ($^{\circ}\text{C}$) with mixed layer depth (dashed line), and **(d)** vertical velocity (m day^{-1}) averaged for Box-L (northwestern Luzon, L in Fig. 1) during 2000–2007. Solid line in **(b)** is 1 mmol N m^{-3} . Solid line in **(c)** is 20° .

An eddy-resolving physical-biological model study

Y. Sasai et al.



Box-V (11°N-15°N, 110°E-114°E)

Fig. 6. Same as for Fig. 5, but for Box-V (southeast Vietnam, V in Fig. 1).

[Title Page](#)

[Abstract](#) [Introduction](#)

[Conclusions](#) [References](#)

[Tables](#) [Figures](#)

[◀](#) [▶](#)

[◀](#) [▶](#)

[Back](#) [Close](#)

[Full Screen / Esc](#)

[Printer-friendly Version](#)

[Interactive Discussion](#)



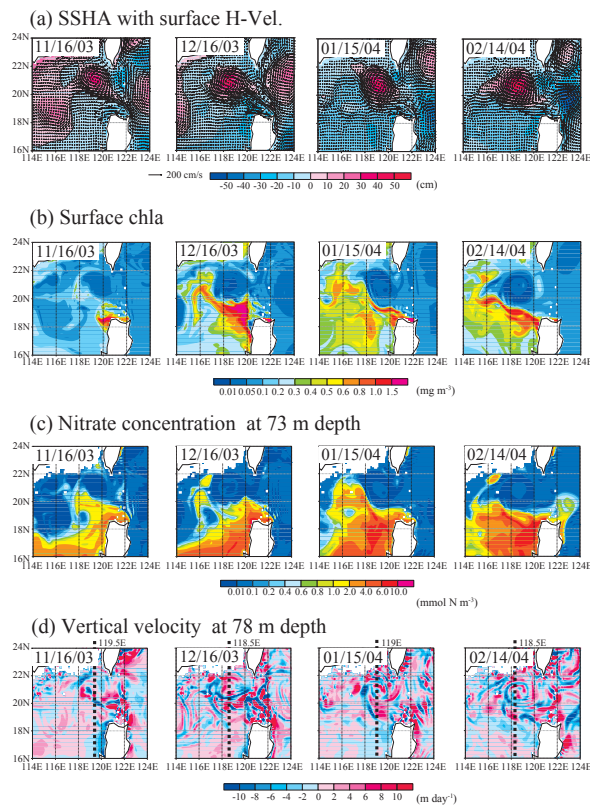


Fig. 7. Snapshots of simulated **(a)** sea surface height anomaly (color, cm) and surface horizontal velocity (vectors, cm s^{-1}), **(b)** surface chlorophyll concentration (mg m^{-3}), **(c)** nitrate concentration at 73 m depth (mmol N m^{-3}), and **(d)** vertical velocity at 78 m depth (m day^{-1}) from November 2003 to February 2004 in the northeastern South China Sea. Dashed line in **(d)** is the center of anticyclonic eddy location.

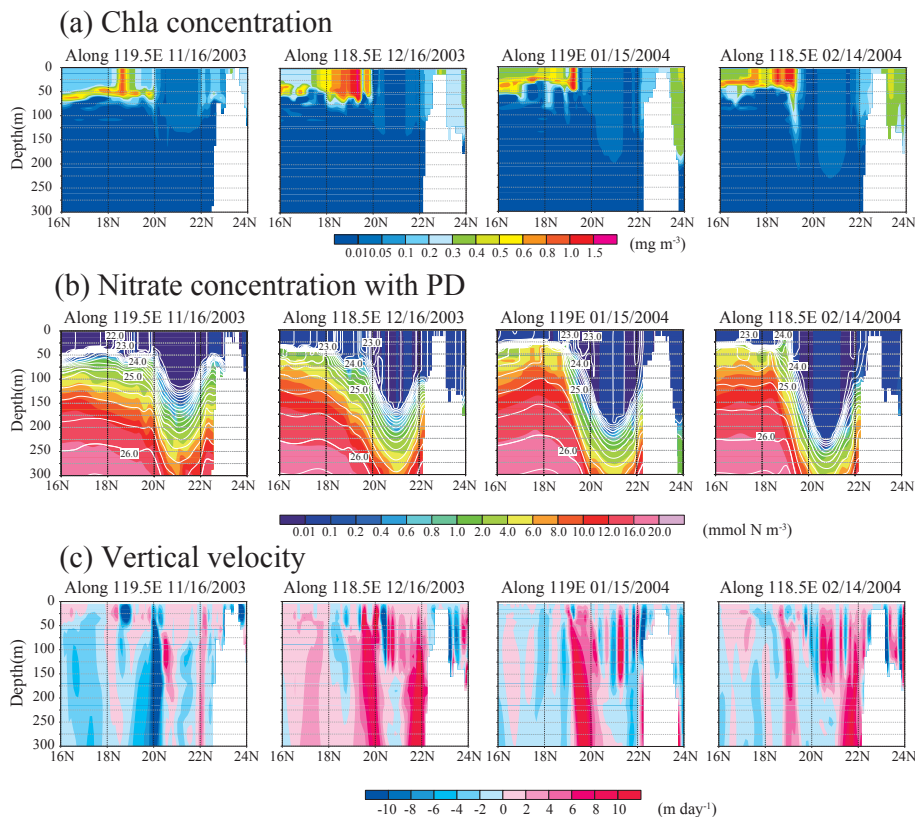


Fig. 8. Vertical distributions of snapshots of simulated **(a)** chlorophyll concentration (mg m^{-3}), **(b)** nitrate concentration (color, mmol N m^{-3}) and potential density (contour), and **(c)** vertical velocity (m day^{-1}) from November 2003 to February 2004 along the center of anticyclonic eddy (dashed line in Fig. 7d). Contour interval in **(b)** is 0.2.

An eddy-resolving physical-biological model study

Y. Sasai et al.

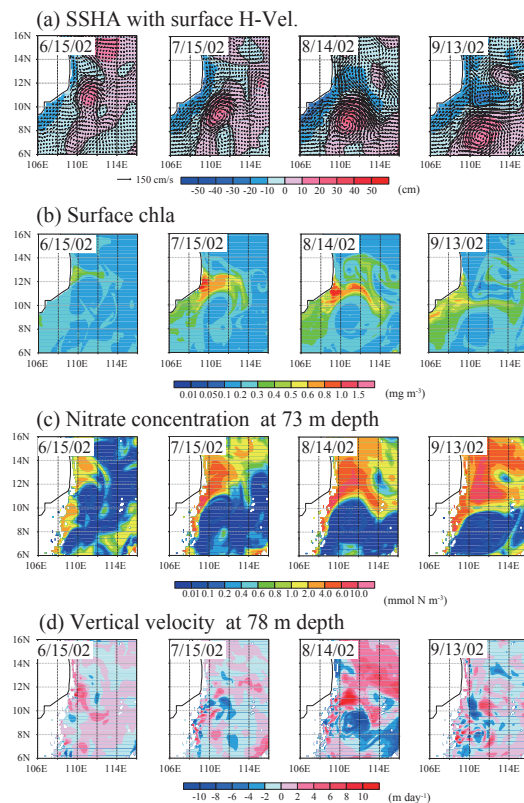


Fig. 9. Snapshots of simulated **(a)** sea surface height anomaly (color, cm) and surface horizontal velocity (vectors, cm s^{-1}), **(b)** surface chlorophyll concentration (mg m^{-3}), **(c)** nitrate concentration at 73 m depth (mmol N m^{-3}), and **(d)** vertical velocity at 78 m depth (m day^{-1}) from June 2002 to September 2002 in the southwestern South China Sea.

Title Page

Abstract

Introduction

Conclusions

References

Tables

Figures

◀

▶

◀

▶

Back

Close

Full Screen / Esc

Printer-friendly Version

Interactive Discussion



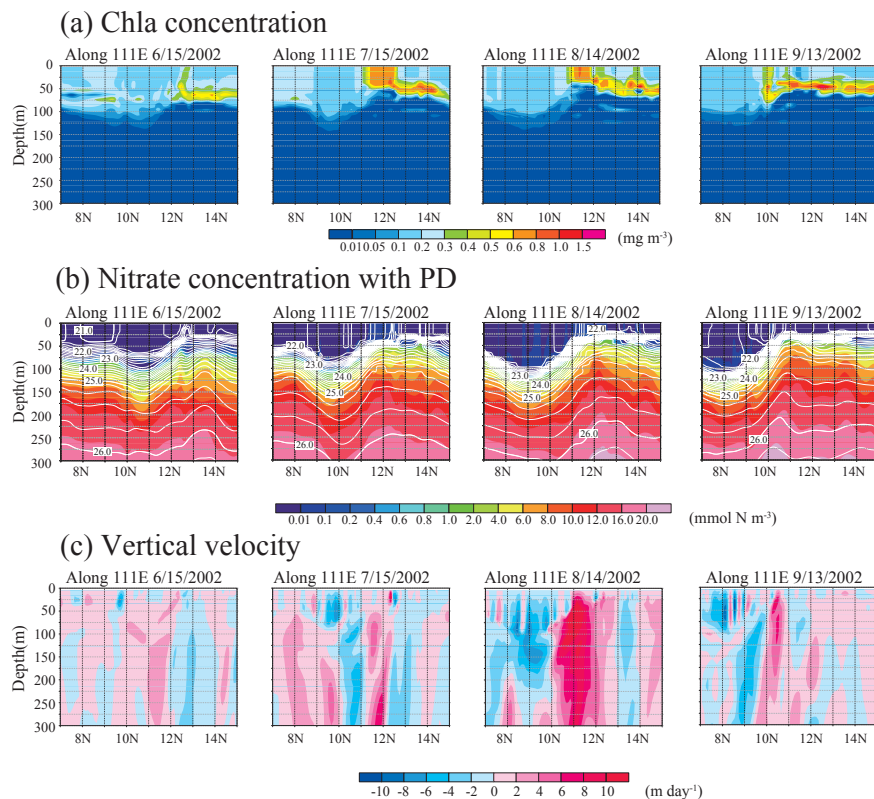


Fig. 10. Vertical distributions of snapshots of simulated **(a)** chlorophyll concentration (mg m^{-3}), **(b)** nitrate concentration (color, mmol N m^{-3}) and potential density (contour), and **(c)** vertical velocity (m day^{-1}) from June 2002 to September 2002 along 111°E in the southwestern South China Sea. Contour interval in **(b)** is 0.2.